

Aqueous Humor Natural Convection of the Human Eye induced by Electromagnetic Fields: In the Supine Position

Teerapot Wessapan

School of Aviation, Eastern Asia University, Pathumthani 12110, Thailand

Email: teerapot@yahoo.com

Phadungsak Rattanadecho

Department of Mechanical Engineering, Faculty of Engineering, Thammasat University,

Pathumthani 12120, Thailand

Email: ratphadu@engr.tu.ac.th

Abstract—This study presents the simulation of the specific absorption rate (SAR), fluid flow and heat transfer in an anatomical human eye exposed to EM fields in the supine position. In this study, the frequencies of 900 and 1800 MHz were chosen for our simulations. This work focuses on the aqueous humor natural convection of the lying human eye induced by electromagnetic (EM) fields. In this study, the effect of operating frequency on the SAR, fluid flow and heat transfer in the eye was systematically investigated. The SAR value and the temperature distribution in various tissues in the eye during exposure to EM fields were obtained by numerical simulation of EM wave propagation and a heat transfer model was then developed based on the natural convection and porous media theories. The findings demonstrate the potential of aqueous humor natural convection in enhancing heat transfer of the eye in the supine position.

Index Terms—electromagnetic fields, heat transfer, specific absorption rate, human eye, natural convection

I. INTRODUCTION

Since the human eye is one of the most sensitive organs to the EM radiation. The high intensity EM fields can lead to a number of ocular effects. However, the resulting thermo-physiologic response of the eye to EM fields is still not well understood. In order to gain insight into the phenomena of heat and mass transfer in the eye concerned with the temperature distribution induced by EM fields, a detailed knowledge of the absorbed power distribution as well as the temperature distribution is necessary. Therefore, this study investigates the ocular effects occurred during exposure to EM fields. The severity of these effects produced by increasing a small temperature can cause eyesight to worsen. There have been medical case reports of the formation of cataracts in humans following accidental exposure to microwave radiation [1]. Actually, a small temperature increase of 3-

5 °C in the eye leads to induce cataracts formation [2]. Additionally, it is reported that the temperature above 41°C is necessary for production of posterior lens opacities [3].

The topic of temperature increase in human tissue when exposed to EM fields, particularly those radiated to the eye, has been of interest for many years. Recently, the modeling of heat transport in human tissue has been investigated by many researchers [4]-[17]. The thermal modeling of human tissue is important as a tool to investigate the effect of external heat sources and to predict the abnormalities in the tissue. In the past, most studies of heat transfer analysis in the eye used heat conduction equation [4]-[10]. Some studies carried out on the natural convection in the eye based on heat conduction model [11], [12]. Ooi and Ng [12], [13] studied the effect of aqueous humor (AH) hydrodynamics on the heat transfer in the eye based on heat conduction model. Meanwhile, the bioheat equation, introduced by Pennes [14], [15] based on the heat diffusion equation for a blood perfused tissue, is used for modeling of the heat transfer in the eye as well [16], [17]. Ooi and Ng also developed a three-dimensional model of the eye [18], extending their two-dimensional model [17]. Recently, porous media models have been utilized to investigate the transport phenomena in biological media instead of a simplified bioheat model [19]-[21]. Shafahi and Vafai [22] proposed the porous media along with a natural convection model to analyze the eye thermal characteristics during exposure to thermal disturbances. The other research groups have been tried to conduct the advanced model using a coupled model of heat and EM dissipation in the eye [6]-[10]. Ooi et al. have been tried to conduct the advanced model using the coupled model of heat and laser irradiation in the eye [23]. Results from a similar model of Ooi *et al.* [23] for various applications were also presented in continuation [24]-[27]. Wessapan *et al.* [28] investigated the SAR and temperature distributions in the eye during exposed to EM waves at 900 MHz using the porous media theory.

Most previous studies of the interaction between the EM fields and the eye mainly focused on SAR. They have not been considered heat transfer causing an incomplete analysis of results. Therefore, the modeling of the heat transport is needed to completely explain the actual process of interaction between the EM fields and the eye. Although the porous media and natural convection models of the eye have been used in the previous biomedical studies [11], [12], [30], most studies of the human eye exposed to the EM fields, especially at different frequencies, have not been considering the porous media and natural convection approaches is sparse or non-existent.

This study presents the simulation of the SAR, fluid flow and temperature distributions in an anatomical human eye exposed to EM fields in the supine position. The work described in this paper is substantially extended from our previous work [28] by further enhancing the focus on the transport phenomena in the eye of lying human. In this study, a two-dimensional human eye model was used to simulate the SAR and temperature distributions in the eye model. The EM wave propagation in the eye was investigated by using Maxwell's equations. An analysis of the heat transfer in the eye exposed to TM-mode of EM fields at different frequencies was investigated using a developed heat transfer model (included the conduction and natural convection heat transfer modes) [22]. In the eye model of lying human, the effect of operating frequency on the SAR, fluid flow and temperature distributions in the eye is systematically investigated. The SAR and temperature distributions in various parts of the eye during exposure to EM fields of 900 and 1800 MHz are obtained by numerical simulation of the EM wave propagation and heat transfer equations.

II. FORMULATION OF THE PROBLEM

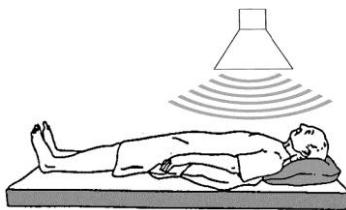


Figure 1. EM fields from an EM radiation device radiated to a supine human body.

Fig. 1 shows the radiation of the EM fields from an EM radiation device to the eye of lying human. These EM fields fall on the eye that causes heating in the deeper tissue, which leads to tissue damage and cataract

formation. Due to ethical consideration, exposing the human to EM fields for experimental purposes is limited. It is more convenient to develop a realistic human eye model through the numerical simulation. A highlight of this work is the illustration of the transport phenomena, including the heat and mass transfer in the eye during exposure to EM fields at different frequencies. The analyses of the SAR and the heat transfer in the eye exposed to EM fields will be illustrated in Sec. 3. The system of governing equations as well as the initial and boundary conditions are solved numerically using the finite element method (FEM).

III. METHODS AND MODEL

The first step in evaluating the effects of a certain exposure to EM fields in the eye is to determine the induced internal EM fields and its spatial distribution. Thereafter, EM energy absorption which results in temperature increase in the eye and other interactions will be able to be considered.

A. Physical Model

In this study, the two-dimensional model of the eye, which follows the physical model in the previous research [22], is developed. Fig. 2 shows the two-dimensional eye model used in this study. This model comprises 7 types of tissue including cornea, anterior chamber, posterior chamber, iris, sclera, lens and vitreous. These tissues have the different dielectric and thermal properties. In the sclera layer, there are two more layers known as the choroid and retina which are relatively thin compared to the sclera. To simplify the problem, these layers are assumed to be homogeneous. The iris and sclera, which have the same properties, are modeled together as one homogenous region [12]. The dielectric and thermal properties of tissue are given in Tables I and II, respectively. Each tissue is assumed to be homogeneous and electrically as well as thermally isotropic.

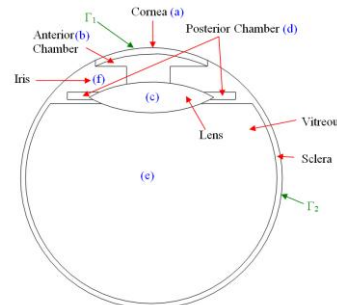


Figure 2. Human eye vertical cross section [22].

TABLE I. DIELECTRIC PROPERTIES OF TISSUES AT 900 MHz AND 1800 MHz [29]-[31]

	Frequency: 900		Frequency: 1800	
	ϵ_r	σ (S/m)	ϵ_r	σ (S/m)
Cornea (a)	52.0	1.85	55.0	2.32
Anterior Chamber (b)	73.0	1.97	75.0	2.40
Lens (c)	51.3	0.89	41.1	1.29
Posterior Chamber (d)	73.0	1.97	75.0	2.40
Vitreous (e)	74.3	1.97	73.7	2.33
Sclera (f)	52.1	1.22	52.7	1.68
Iris (f)	52.1	1.22	52.7	1.68

TABLE II. THERMAL PROPERTIES OF THE EYE [12]

Tissue	ρ (kg/m ³)	k (W/m ² °C)	C_p (J/kg°C)	μ (N s/m ²)	β (1/K)
Cornea (a)	1050	0.58	4178	-	-
Anterior Chamber (b)	996	0.58	3997	0.00074	0.000337
Lens (c)	1000	0.4	3000	-	-
Posterior Chamber (d)	996	0.58	3997	-	-
Vitreous (e)	1100	0.603	4178	-	-
Sclera (f)	1050	1.0042	3180	-	-
Iris (f)	1050	1.0042	3180	-	-

B. Equations for EM Wave Propagation Analysis

The mathematical models are developed to predict the electric fields and the SAR with respect to the temperature gradient in the eye. To simplify the problem, the following assumptions are made:

- 1) The EM wave propagation is modeled in two dimensions.
- 2) The eye in which the EM waves interact with the eye proceeds in the open region.
- 3) The free space is truncated by scattering boundary condition.
- 4) The model assumes that dielectric properties of each tissue are constant.
- 5) In the eye, the EM waves are characterized by transverse magnetic fields (TM-mode).

The EM wave propagation in the eye is calculated using Maxwell's equations which mathematically describe the interdependence of the EM waves. The general form of Maxwell's equations is simplified to demonstrate the EM fields penetrated in the eye as the following equation:

$$\nabla \times \left(\left(\epsilon_r - \frac{j\sigma}{\omega\epsilon_0} \right)^{-1} \nabla \times H_z \right) - \mu_r k_0^2 H_z = 0 \quad (1)$$

where H is the magnetic field (A/m), μ_r is the relative magnetic permeability, ϵ_r is the relative dielectric constant, $\epsilon_0 = 8.8542 \times 10^{-12}$ F/m is the permittivity of free space, k_0 is the free space wave number (m⁻¹).

Boundary condition for wave propagation analysis

EM energy is emitted by an EM radiation device and falls on the eye with a particular power density. Therefore, boundary condition for solving EM wave propagation is described as follows:

It is assumed that the uniform wave flux falls on the left side of the eye. Therefore, at the left boundary of the considered domain, an EM simulator employs TM wave propagation port with specified power density,

$$S = [(E - E_1) \cdot E_1] / E_1 \cdot E_1 \quad (2)$$

Boundary conditions along the interfaces between different mediums, for example, between air and tissue or tissue and tissue, are considered as continuity boundary condition,

$$n \times (E_1 - E_2) = 0 \quad (3)$$

The outer sides of the calculated domain, i.e., free space, are considered as scattering boundary condition [25],

$$n \times (\nabla \times E_z) - jkE_z = -jk(1 - k \cdot n)E_{0z} \exp(-jk \cdot r) \quad (4)$$

where k is the wave number (m⁻¹), σ is the electrical conductivity (S/m), n is the normal vector, $j = \sqrt{-1}$, and E_0 is the incident plane wave (V/m).

C. Interaction of EM Fields and Human Tissues

Interaction of EM fields with biological tissue can be defined in the term of the SAR. When the EM waves propagate through the tissue, the energy of EM waves is absorbed by the tissue. The SAR is defined as power dissipation rate normalized by material density [21]. The SAR is given by,

$$SAR = \frac{\sigma}{\rho} |E|^2 \quad (5)$$

where E is the electric field intensity (V/m), σ is the electric conductivity (S/m), and ρ is the tissue density (kg/m³).

D. Equations for Heat Transfer and Flow Analysis

To solve the thermal problem, the coupled effects of the EM wave propagation and the unsteady bioheat transfer are investigated. The temperature distribution is corresponded to the SAR. This is because the SAR in the eye distributes owing to energy absorption. Thereafter, the absorbed energy is converted to thermal energy, which increases the tissue temperature.

Heat transfer analysis of the eye is modeled in two dimensions. To simplify the problem, the following assumptions are made:

- 1) The Human tissue is a bio-material with constant thermal properties.
- 2) There is no phase change of substance in the tissue.
- 3) There is a local thermal equilibrium between the blood and the tissue.
- 4) There is no chemical reaction in the tissue.

This study utilized the pertinent thermal model based on the porous media theory [22] to investigate the heat transfer behavior of the eye when exposed to the EM fields.

In this study, the motion of fluid is considered only inside the anterior chamber [12]. There is a blood flow in the iris/sclera part, which plays a role to adjust the eye temperature with the rest of the body [22]. For the rest parts, the metabolic heat generation is neglected based on the fact that these comprise mainly water [12]. The equation governing the flow of heat in cornea, posterior chamber, lens and vitreous are resembled the classical heat conduction equation given in Eq. (6).

$$\rho_i C_i \frac{\partial T_i}{\partial t} = \nabla \cdot (k_i \nabla T_i) + Q_{ext} \quad ; i = a, c, d, e \quad (6)$$

This model accounts for the existence of AH in the anterior chamber. The heat transfer process consists of both the conduction and natural convections, which can be written as follows:
Continuity equation:

$$\nabla \cdot u_i = 0 \quad ; \quad i=b \quad (7)$$

Momentum equation:

$$\rho_i \frac{\partial u_i}{\partial t} + \rho_i u_i \nabla \cdot u_i = -\nabla p_i + \nabla \cdot [\mu(\nabla u_i + \nabla u_i^T)] + \rho_i g \beta_i (T_i - T_{ref}) \quad ; i=b \quad (8)$$

where i denotes each subdomain in the eye model as shown in Fig. 2, ρ is the tissue density (kg/m^3), β is the volume expansion coefficient ($1/\text{K}$), u is the velocity (m/s), p is the pressure (N/m^2), μ is the dynamic viscosity of AH (N.s/m^2), t is the time, T is the tissue temperature (K), and T_{ref} is the reference temperature considered here is 37°C . The effects of buoyancy due to the temperature gradient are modeled using the Boussinesq approximation which states that the density of a given fluid changes slightly with temperature but negligibly with pressure [12].

Energy equation:

$$\rho_i C_i \frac{\partial T_i}{\partial t} - \nabla \cdot (k_i \nabla T_i) = -\rho C_i u_i \cdot \nabla T_i + Q_{ext} \quad ; i=b \quad (9)$$

The sclera/iris is modeled as a porous medium with the blood perfusion, which assumes that local thermal equilibrium exists between the blood and the tissue. The blood perfusion rate used is $0.0041/\text{s}$. A modified Pennes' bioheat equation [22], [31] is used to calculate the temperature distribution in the sclera/iris.

$$(1 - \varepsilon) \rho_i C_i \frac{\partial T_i}{\partial t} = \nabla \cdot ((1 - \varepsilon) k_i \nabla T_i) + \rho_b C_b \omega_b (T_b - T_i) + Q_{ext} \quad ; i=f \quad (10)$$

where C is the heat capacity of tissue (J/kg K), k is the thermal conductivity of tissue (W/m K), T_b is the temperature of blood (K), ρ_b is the density of blood (kg/m^3), C_b is the specific heat capacity of blood (J/kg K), ω_b is the blood perfusion rate ($1/\text{s}$), and Q_{ext} is the external heat source term (EM heat-source density) (W/m^3).

In the analysis, the porosity (ε) used is assumed to be 0.6. The heat conduction between the tissue and the blood

flow is approximated by the blood perfusion term, $\rho_b C_b \omega_b (T_b - T)$.

The external heat source term is equal to the resistive heat generated by the EM fields (EM power absorbed), which defined as

$$Q_{ext} = \frac{1}{2} \sigma_{tissue} |E|^2 = \frac{\rho}{2} \cdot SAR \quad (11)$$

where σ_{tissue} is the electric conductivity of tissue (S/m).

Boundary condition for heat transfer analysis

The heat transfer analysis excluding the surrounding space is considered only in the eye. The cornea surface is considered as the convective, radiative, and evaporative boundary conditions.

$$-n \cdot (-k \nabla T) = h_{am} (T_i - T_{am}) + \varepsilon \sigma (T_i^4 - T_{am}^4) + e$$

$$\text{on } \Gamma_1 \quad i = a \quad (12)$$

where Γ_1 is the external surface area corresponding to section i , e is the tear evaporation heat loss (W/m^2), T_{am} is the ambient temperature (K), h_{am} is the convection coefficient ($\text{W/m}^2 \cdot \text{K}$).

The temperature of blood generally assumed to be the same as the body core temperature causes heat to be transferred into the eye [12]. The surface of the sclera is assumed to be a convective boundary condition

$$-n \cdot (-k_i \nabla T_i) = h_b (T_b - T_i) \quad \text{on } \Gamma_2 \quad i = f \quad (13)$$

where h_b is the convection coefficient of blood ($65 \text{ W/m}^2 \cdot \text{K}$). Γ_1 and Γ_2 are the corneal surface and sclera surface of the eye, respectively.

E. Calculation Procedure

In this study, the finite element method is used to analyze the transient problems. The computational scheme is to assemble finite element model and compute a local heat generation term by performing an EM calculation using tissue properties. In order to obtain a good approximation, a fine mesh is specified in the sensitive areas. This study provides a variable mesh method for solving the problem as shown in Fig. 3. The system of governing equations as well as the initial and boundary conditions are then solved.

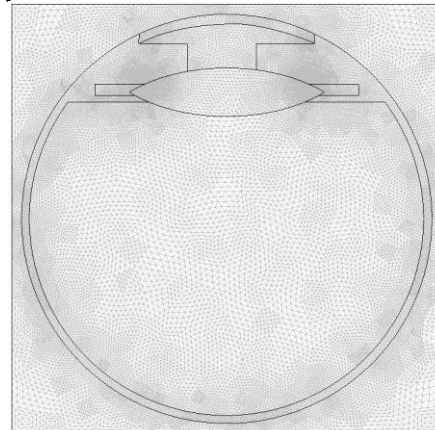


Figure 3. A two-dimensional finite element meshes of the eye model.

The 2D model is discretized using triangular elements and the Lagrange quadratic is then used to approximate the temperature and SAR variations across each element. The convergence test is carried out to identify the suitable number of elements required. This convergence test leads to the grid with approximately 10,000 elements. It is reasonable to assume that, at this element number, the accuracy of the simulation results is independent from the number of elements.

IV. RESULTS AND DISCUSSION

Since most GSM networks use frequencies in the 900 and 1800 MHz spectrum, therefore, in this analysis, the effects of these operating frequencies on distributions of SAR and temperature in the eye are systematically investigated. In this study, the coupled model of the EM and thermal fields are solved numerically. For the simulation, the dielectric and thermal properties are directly taken from Tables 1 and 2, respectively.

A. Verification of the Model

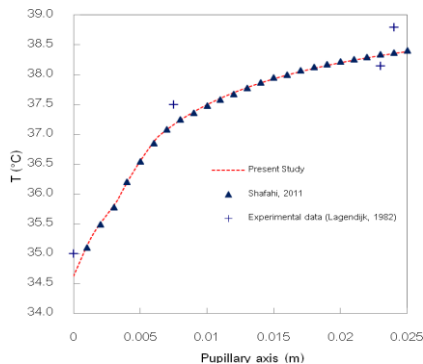


Figure 4. Comparison of the calculated temperature distribution to the temperature distribution obtained by Shafahi and Vafai [22], and the Legendijk's experimental data [4]; $h_{am}=20\text{W/m}^2\cdot\text{K}$ and $T_{am}=25\text{ }^\circ\text{C}$.

In order to verify the accuracy of the present numerical models, the case without EM fields of the simulated results from this study are validated against the numerical results with the same geometric model obtained by Shafahi and Vafai [22]. Moreover, the numerical results are then compared to the experimental results of the rabbit obtained from Legendijk [4]. The validation case assumes that the rabbit body temperature is $38.8\text{ }^\circ\text{C}$, the tear evaporation heat loss is 40 W/m^2 , the ambient temperature is $25\text{ }^\circ\text{C}$, and the convection coefficient of ambient air is $20\text{ W/m}^2\cdot\text{K}$. The results of the selected test case are depicted in Fig. 4 for temperature distribution in the eye. Fig. 4 clearly shows a good agreement of the temperature distribution in the eye between the present solution and that of Shafahi and Vafai [22] and Legendijk [4]. In the figure, the simulated results provides a good agreement with the simulated results obtained from Shafahi and Vafai [22]. This favorable comparison lends confidence in the accuracy of the present numerical model.

B. Electric field Distribution

Fig. 5 shows the simulation of an electric field pattern inside the eye exposed to the EM fields in TM mode

operating at the frequencies of 900 and 1800 MHz propagating along the vertical cross section human eye model. By comparison, the maximum electric field intensity in outer parts of the eye at the frequency of 900 MHz displays a higher value than that of 1800 MHz. The maximum electric field intensities are 391.8 and 231.2 V/m at the frequencies of 900 and 1800 MHz, respectively. The maximum value for the frequency of 900 MHz is in the cornea while for the frequency of 1800 MHz is in the lens. Mathematically, this result corresponds to Eq. (1) and the dielectric properties (ϵ_r) in Table I show that the frequency of 900 MHz has lower dielectric properties of cornea, while the frequency of 1800 MHz has lower dielectric properties of lens. It is found that these alterations of electric field distribution between the two chosen frequencies vary in extent with the magnitude of the dielectric property and with the standing-wave pattern.

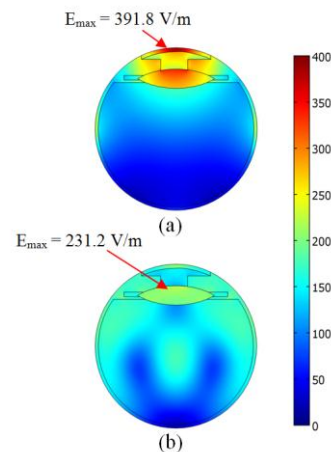


Figure 5. Electric field distribution (V/m) in the eye exposed to the EM power density of 100 mW/cm^2 at the frequencies of (a) 900 MHz and (b) 1800 MHz.

C. SAR Distribution

Fig. 6 shows the SAR distribution evaluated on the vertical cross section of the eye exposed to the EM frequencies of 900 and 1800 MHz. It is evident from the figure that the results of the SAR values in the eye (Fig. 6) are increased corresponding to the electric field intensities (Fig. 5). Besides the electric field intensity, the magnitude of the dielectric and thermal properties in each tissue will directly affect SAR values in the eye. For both frequencies, the highest SAR values are obtained in the region of the corneal surface. In this region, the frequencies of 900 and 1800 MHz display SAR values of 135.2 and 45.9 W/kg, respectively. This is because the cornea has a much higher value of its electrical conductivity (σ) than those of lens and iris. The second main reason is the position of the cornea located close to the exposed surface, at which the electric field intensity is strongest. It is found that the SAR distribution pattern in the eye, which corresponds to Eq. (5), is strongly depended on the effect of the dielectric properties (σ , shown in Table I) and thermal properties (ρ , shown in Table II). Moreover, the SAR pattern at the frequency of 1800 MHz shows a greater value of the EM power

absorption in the deep part of the eye, with less surface heating, compared to those of 900 MHz.

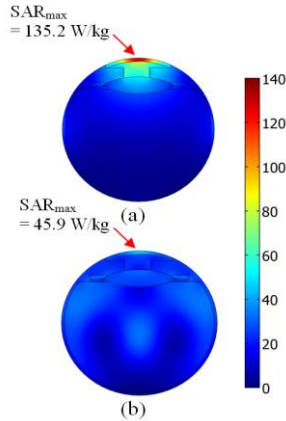


Figure 6. SAR distribution (W/kg) in the eye exposed to the EM power density of 100 mW/cm² at the frequencies of (a) 900 MHz and (b) 1800 MHz.

D. Velocity Fields and Temperature Distributions

In this study, the effect of an ambient temperature variation have been neglected in order to gain insight into the interaction between the EM fields and the tissue as well as the correlation between the SAR and the heat transfer mechanism. For this reason, the ambient temperature has been set to the human body temperature of 37 °C, and the tear evaporation has been neglected. Moreover, the effect of thermoregulation mechanisms has also been neglected due to the small temperature increase occurred during exposure process. The convective coefficient due to the blood flow inside the sclera is set to 65 W/m².K [12].

Fig. 7 shows the circulatory patterns in the anterior chamber in the eye exposed to the EM frequencies of 900 and 1800 MHz at various times. These patterns vary corresponding to the temperature gradient in the eye. Therefore, in the case of a lower temperature gradient, the circulatory patterns have a lower speed, where a circulatory pattern with a higher temperature gradient flows faster. For the 900 MHz frequency, at the early stage ($t=10s$) a counterclockwise circulation thus appears in the anterior chamber, shown in Fig. 7a. This seemed to imply that the heat gradually travels inward passes through the front of the eye to the lens corresponding to the higher SAR value at the cornea surface (Fig. 6a). Later, it is found that the natural convection and formation of two circulatory patterns with opposite direction in the anterior chamber, shown in Fig. 7a, play important roles on the cooling processes in the eye, especially in the inner corneal surface. It is observed that a large temperature gradient is significantly produced by the EM fields after 10 minutes. The circulation pattern implies that the generated heat in the anterior chamber is transferred outward from the lens surface. While for the 1800 MHz frequency, at the early stage the formation of two circulatory patterns with opposite direction in the anterior chamber is occurred in the inward direction. Surprisingly, after 60s, the circulatory patterns in the reverse direction thus appear in the anterior chamber,

shown in Fig. 7b. The direction of heat transfer is to reverse outward from the lens surface. In the stage of heating (after 60 s), the effect of convective flow becomes stronger and plays a more important role, especially at the center region of the anterior chamber. However, at the peripheral region of the anterior chamber where the convection flow is small, temperature distributions are primarily governed by the conduction mode. At the steady state, the flow pattern is symmetrical between left and right sides for both frequencies. The flow fields are in the same direction but the magnitudes of velocity are clearly different. The circulation pattern in each case significantly different from each other, this is because each case exhibited a different heating pattern.

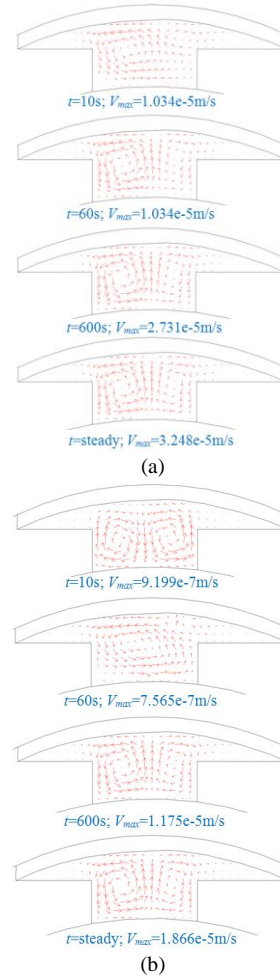


Figure 7. The velocity fields inside the anterior chamber at various time exposed to the EM power density of 100 mW/cm² at the frequencies of (a) 900 MHz and (b) 1800 MHz.

Fig. 8 shows the temperature distribution in the vertical cross section human eye at various time exposed to the EM frequencies of 900 (Fig. 8a) and 1800 MHz (Fig. 8b). For the eye exposed to the EM fields for a period of time, the temperature in the eye (Fig. 8) is increased corresponding to the SAR (Fig. 6). This is because the electric fields in the eye attenuate owing to the energy absorbed and thereafter the absorbed energy is converted to thermal energy, which increases the eye temperature.

For the 900 MHz frequency, even though the maximum values of the electric fields (Fig. 5a) and the

SAR (Fig. 6a), are the cornea, the highest temperature is the anterior chamber (Fig. 8a). This is owing to the extensive penetration of the EM power of the internal regions and the higher dielectric properties (ϵ_r) of the anterior chamber. This higher dielectric property of the anterior chamber represents the stronger absorption ability of EM fields than those of cornea and lens. Moreover, the outer corneal surface has a lower temperature than that of the anterior chamber, even if it has higher SAR value (Fig. 6a). This is because, in this area, the generated heat is dissipated to the ambient via convection and radiation.

While for the 1800 MHz frequency, beside the cornea and lens, the high value of the electric fields is the middle of the vitreous and peripheral vitreous. This is owing to the constructive interference between the forward and reflected waves of the higher frequency of 1800 MHz results in standing wave patterns forming in the EM fields (Fig. 7b) in the vitreous area. This high electric field intensity increases the amount of energy absorption in the vitreous area (Fig. 8b) and consequently causes the temperature to rise (Fig. 9b). In this case, the maximum temperature increase in the

peripheral vitreous area has a lower level than that of the middle of the vitreous even if the peripheral vitreous area also has high electric field intensity and the SAR value also. This is due to the presence of blood perfusion in the sclera tissue, which covers an internal surface area of the eye. This blood perfusion provides buffer characteristic to the eye temperature and plays important roles on the cooling processes in the peripheral vitreous area.

A longer exposure time resulted in a higher heat accumulation inside the eye, thereby increasing its temperature. By using the operating frequency of 900 MHz, the maximum temperatures increase are 0.216, 0.849, 2.433, and 3.052 °C for the exposure times of 10s, 60s, 600s, and at steady-state conditions of 3600s, respectively. By using the operating frequency of 1800 MHz, the maximum temperatures increase are 0.1, 0.417, 2.068, and 40.323 °C for the exposure times of 10s, 60s, 600s, and at steady-state conditions of 3600s, respectively.

In this study, the maximum temperature increase in the eye exposed to the EM fields with the power density of 100 mW/cm² at the frequencies of 900 and 1800 MHz are 3.052 and 3.323 °C, respectively.

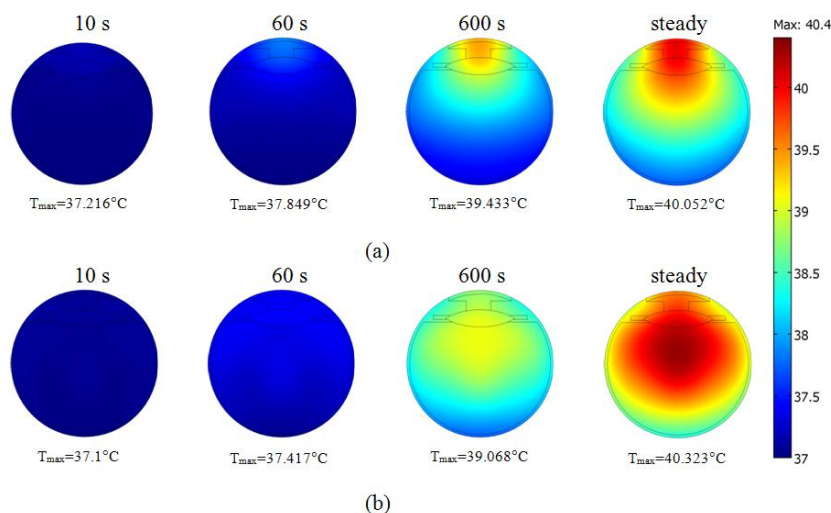


Figure 8. The temperature distribution in the eye at various time exposed to the EM power density of 100 mW/cm² at the frequencies of (a) 900 MHz and (b) 1800 MHz.

V. CONCLUSIONS

In this study, the aqueous humor natural convection of the lying human eye induced by electromagnetic (EM) fields is systematically investigated. From the results, the electric field distributions show a strong dependence on the dielectric properties of the tissue. The results of the SAR values are increased corresponding to the electric field intensities. Besides the electric field intensity, the magnitude of the dielectric and thermal properties in each tissue will directly affect the SAR values in the eye. It is found that the convective heat transfer in the anterior chamber plays a significant role in transferring heat. This will allow a better understanding of the realistic situation of the interaction between the EM fields and the eye.

ACKNOWLEDGMENT

This work has been financially supported by the Thailand Research Fund (TRF), the Commission on Higher Education (CHE) and Eastern Asia University.

REFERENCES

- [1] A. F. Emery, P. Kramar, A. W. Guy, and J. C. Lin, "Microwave induced temperature rises in rabbit eyes in cataract research," *ASME J. Heat Transfer*, vol. 97, pp. 123–128, 1975.
- [2] C. Buccella, V. D. Santis, and M. Feliaiani, "Prediction of temperature increase in human eyes due to RF sources," *IEEE Trans. Electromagn. Compat.*, vol. 49, no. 4, pp. 825–833, 2007.
- [3] J. C. Lin, "Cataracts and cell-phone radiation," *IEEE Antennas and Propagation*, vol. 45, no. 1, pp. 171–174, 2003.
- [4] J. J. W. Lagendijk, "A mathematical model to calculate temperature distribution in human and rabbit eye during

- hyperthermic treatment," *Physics in Medicine and Biology*, vol. 27, pp. 1301–1311, 1982.
- [5] J. Scott, "A finite element model of heat transport in the human eye," *Physics in Medicine and Biology*, vol. 33, pp. 227–241, 1988.
- [6] J. Scott, "The computation of temperature rises in the human eye induced by infrared radiation," *Physics in Medicine and Biology*, vol. 33, pp. 243–257, 1988.
- [7] E. H. Amara, "Numerical investigations on thermal effects of laser–ocular media interaction," *Int. J. Heat Mass Transfer*, vol. 38, pp. 2479–2488, 1995.
- [8] A. Hirata, S. Matsuyama, and T. Shiozawa, "Temperature rises in the human eye exposed to EM waves in the frequency range 0.6–6 GHz," *IEEE Trans. Electromagnetic Compat.*, vol. 42, no. 4, pp. 386–393, 2000.
- [9] K. J. Chua, J. C. Ho, S. K. Chou, and M. R. Islam, "On the study of the temperature distribution within a human eye subjected to a laser source," *Int. Commun. Heat Mass Transfer*, vol. 32, pp. 1057–1065, 2005.
- [10] W. Limtrakarn, S. Reepolmaha, and P. Dechaumphai, "Transient temperature distribution on the corneal endothelium during ophthalmic phacoemulsification: A numerical simulation using the nodeless variable element," *Asian Biomedicine*, vol. 4, no. 6, pp. 885–892, 2010.
- [11] S. Kumar, S. Acharya, R. Beuerman, and A. Palkama, "Numerical solution of ocular fluid dynamics in a rabbit eye: Parametric effects," *Ann. Biomed. Eng.*, vol. 34, pp. 530–544, 2006.
- [12] E. Ooi and E. Y. K. Ng, "Simulation of aqueous humor hydrodynamics in human eye heat transfer," *Comput. Biol. Med.*, vol. 38 pp. 252–262, 2008.
- [13] E. H. Ooi and E. Y. K. Ng, "Effects of natural convection inside the anterior chamber," *International Journal for Numerical Methods in Biomedical Engineering*, vol. 27, pp. 408–423, 2011.
- [14] H. H. Pennes, "Analysis of tissue and arterial blood temperatures in the resting human forearm," *J. Appl. Physiol.*, vol. 1, pp. 93–122, 1948.
- [15] H. H. Pennes, "Analysis of tissue and arterial blood temperatures in the resting human forearm," *J. Appl. Physiol.*, vol. 85, no. 1, pp. 5–34, 1998.
- [16] V. M. M. Flyckt, B. W. Raaymakers, and J. J. W. Lagendijk, "Modeling the impact of blood flow on the temperature distribution in the human eye and the orbit: Fixed heat transfer coefficients versus the penne's bioheat model versus discrete blood vessels," *Physics in Medicine and Biology*, vol. 51, pp. 5007–5021, 2006.
- [17] E. Y. K. Ng and E. H. Ooi, "FEM simulation of the eye structure with bioheat analysis," *Comput. Methods Programs Biomed.*, vol. 82, pp. 268–276, 2006.
- [18] E. H. Ooi and E. Y. K. Ng, "Ocular temperature distribution: A mathematical perspective," *J Mech Med Biol*, vol. 9, pp. 199–227, 2009.
- [19] A. Nakayama and F. Kuwahara, "A general bioheat transfer model based on the theory of porous media," *Int. J. Heat Mass Transfer*, vol. 51, pp. 3190–3199, 2008.
- [20] S. Mahjoob and K. Vafai, "Analytical characterization of heat transfer through biological media incorporating hyperthermia treatment," *Int. J. Heat Mass Transfer*, vol. 52, pp. 1608–1618, 2009.
- [21] K. Khanafer and K. Vafai, "Synthesis of mathematical models representing bioheat transport," *Advances in Numerical Heat Transfer*, vol. 3, pp. 1–28, 2009.
- [22] M. Shafahi and K. Vafai, "Human eye response to thermal disturbances," *ASME J. Heat Transfer*, vol. 133, pp. 011009, 2011.
- [23] E. H. Ooi, W. T. Ang, and E. Y. K. Ng, "A boundary element model of the human eye undergoing laser thermokeratoplasty," *Computers in Biology and Medicine*, vol. 28, pp. 727–738, 2008.
- [24] E. H. Ooi, W. T. Ang, and E. Y. K. Ng, "A boundary element model for investigating the effects of eye tumor on the temperature distribution inside the human eye," *Computers in Biology and Medicine*, vol. 28, pp. 727–738, 2009.
- [25] J. H. Tan, E. Y. K. Ng, U. R. Acharya, and C. Chee, "Study of normal ocular thermogram using textural parameters," *Infrared Physics & Technology*, vol. 53, pp. 120–126, 2010.
- [26] J. H. Tan, E. Y. K. Ng, and U. R. Acharya, "Evaluation of tear evaporation from ocular surface by functional infrared thermography," *Medical Physics*, vol. 37, pp. 6022–6034, 2010.
- [27] J. H. Tan, E. Y. K. Ng, and U. R. Acharya, "Evaluation of topographical variation in ocular surface temperature by functional infrared thermography," *Infrared Physics & Technology*, vol. 54, pp. 469–477, 2011.
- [28] T. Wessapan and P. Rattanadecho, "Specific absorption rate and temperature increase in human eye subjected to electromagnetic fields at 900 MHz," *ASME J. Heat Transfer*, vol. 134, pp. 091101, 2012.
- [29] P. Bernardi, M. Cavagnaro, S. Pisa, and E. Piuze, "Specific absorption rate and temperature increases in the head of a cellular-phone user," *IEEE Trans. Microw. Theor. Tech.*, vol. 48, no. 7, pp. 1118–1126, 2000.
- [30] S. Park, J. Jeong, and Y. Lim, "Temperature rise in the human head and brain for portable handsets at 900 and 1800 MHz," in *Proc. Fourth International Conference on Microwave and Millimeter Wave Technology*, vol. 1, 2004, pp. 966–969.
- [31] A. Nakayama and F. Kuwahara, "A general bioheat transfer model based on the theory of porous media," *Int. J. Heat Mass Transfer*, vol. 51, pp. 3190–3199, 2008.



Teerapot Wessapan received the Bachelor's degree in Mechanical Engineering from the Srinakharinwirot University, Bangkok, Thailand in March 2002. He received his master's degree in Mechanical Engineering from Kasetsart University, Bangkok, Thailand in 2005. He received Ph.D. degree in Engineering from Thammasat University, Bangkok, Thailand in 2011. His researches involve the numerical analysis of microwave thermal ablation, thermal response of humans exposed to electromagnetic fields, computer simulation of electromagnetic fields. He is now an Assistant Professor of Mechanical Engineering at Eastern Asia University.



Phadungsak Rattanadecho received the Bachelor's degree in Mechanical Engineering from the King Mongkut Institute of Technology Thonburi, Bangkok, Thailand in March 1991. He received the Master's degree in Mechanical Engineering from Chulalongkorn University, Thailand, in March 1994. He received Ph.D. degree in Mechanical Engineering from the Nagaoka University of Technology, Japan, 2002. His researches concern microwave heating/ drying and melting processes in porous medium, numerical analysis of electromagnetic fields (inside multimode cavity), development of numerical schemes based on lattice boltzmann method for flow and dispersion in porous media, heat and mass transport in complexity boundary-layer and so on. He is now a Professor of Mechanical Engineering at Thammasat University.